Local Dark Matter Density from Improved Local Mass Density of Stars and Updated Baryonic Model

A. Lutsenko, G. Carraro, V. Korchagin, R. Tkachenko, K. Vieira

ROTATION CURVE

- HI and CO terminal velocities

(McClure-Griffiths & Dickey 2007, McClure-Griffiths & Dickey 2016, Sofue & Kohno 2025)

- Molecular masers

(Reid et al. 2019)

- Classical Cepheids

(Ablimit et al. 2020)

- Red Giant Branch stars

(Ou et al. 2024)

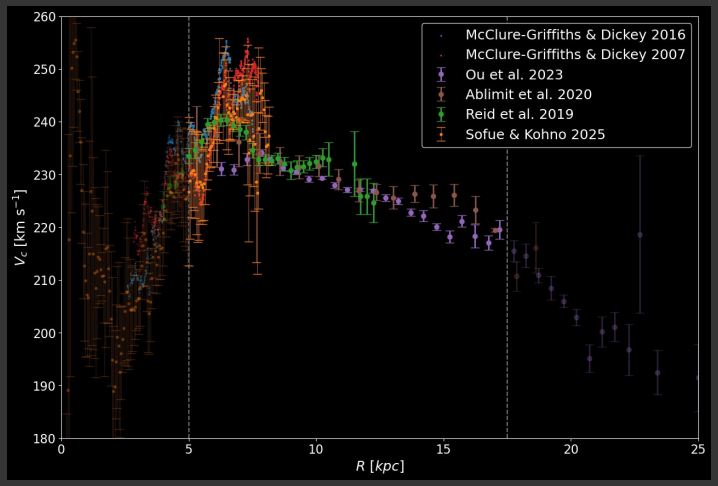

BARYON MODEL

Revised gas model

- Atomic gas disk with flaring
- Molecular gas disk with flaring
- Ionized gas disk (Jo et al 2019)

$$\Sigma = \Sigma_0 \times exp(-\frac{R_m}{R} - \frac{R}{R_d})$$

$$\rho(R,z) = \frac{\Sigma(R)}{4 \cdot h_z(R)} \times sech^2(\frac{z}{2 \cdot h_z(R)})$$

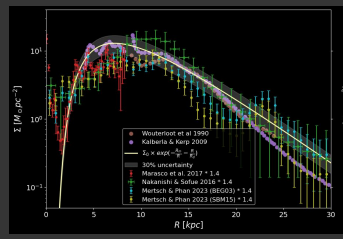

Atomic gas surface density

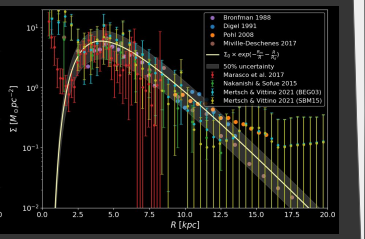

Molecular gas surface density

Star model with recent observations

- Thin disk with flaring

(Vieira et al. 2023, Lian et al. 2025, Sanders & Binney 2015)

- Thick disk with flaring

(Vieira et al. 2023, Lian et al. 2025, Tkachenko et al 2025)

$$\rho_i(R,z) = exp(-\frac{R - R_\odot}{h_R}) \times sech^2(\frac{z}{h_z})$$

Normalised to observationally derived Local Mass Density (Lutsenko et al. 2025)

- Bulge (Dehnen & Binney 1998)

$$\rho_b = \rho_{b0} \left(\frac{\sqrt{R^2 + (\frac{z}{q})^2}}{r_0} \right)^{-\gamma} exp\left(-\frac{R^2 + (\frac{z}{q})^2}{r_t^2} \right)$$

Normalised to inner dynamical mass (Portail et al. 2016)

- Halo (Deason et al. 2011)

DM HALO MODEL

NFW profile
(Navarro, Frenk and White 1997)

$$\rho(r) = \frac{\rho_0}{\frac{r}{r_s}(1 + \frac{r}{r_s})^2}$$

Einasto profile
(Einasto 1965)

$$\rho(r) = \frac{M}{4\pi n h^3 \Gamma(3n)} exp(-(\frac{r}{h})^{1/n})$$

FITTING PROCEDURE

MODEL — Potential reconstruction with Agama (Vasiliev 2019)

Informed priors on baryonic model parameters + wide uniform priors for DM halo parameters

Component	Name	Unit	Range	Description
Atomic gas	$\Sigma_{0,\mathrm{at1}}$	$M_\odot pc^{-2}$	[255.01; 473.50]	Amplitude of the atomic gas density profile
Molecular gas	$\Sigma_{0,\mathrm{at2}}$	$M_\odot pc^{-2}$	[435.79; 1301.27]	Amplitude of the molecular gas density profile
Stellar disks	h_R	kpc	[3.1; 3.8]	Scale length of the thin stellar disk
Stellar disks	h_{z0}	kpc	[0.27, 0.29]	Scale height of the thin stellar disk at R_0
Stellar disks	H_R	kpc	[1.9; 2.3]	Scale length of the thick stellar disk
Stellar disks	H_{z0}	kpc	[0.79, 0.81]	Scale height of the thick stellar disk at R_0
Stellar disks	f_T	–	[0.74, 0.78]	Fraction of thick-to-thin disk density at R_0
Stellar disks	ρ_{tot}	$M_\odot pc^{-3}$	[0.031; 0.052]	Observed local stellar mass density within 100pc
Stellar halo	$M_{\mathrm{at,halo}}$	$M_\odot \times 10^6$	[1.0; 1.8]	Total mass of the stellar halo
Bulge	M_{bulge}	$M_\odot \times 10^9$	[18.0; 19.0]	Normalization of the internal mass
NFW DM Halo	r_s	kpc	[0.1; 100.0]	Scale radius of NFW profile
NFW DM Halo	M_{NFW}	$M_\odot \times 10^6$	[0.1; 100.0]	Mass enclosed within approximately 5.3 scale radius
Einasto DM Halo	M_{Einasto}	$M_\odot \times 10^{11}$	[0.1; 100.0]	Total mass of Einasto DM halo
Einasto DM Halo	h	kpc	[0.1; 100.0]	Scale radius of Einasto DM halo
Einasto DM Halo	n	–	[0.1; 10.0]	Einasto index

DATA

We combine rotation curve measurements from different tracers into a single dataset. Individual measurements were binned with bin size of 0.5 kpc, with per-bin weighting adjusted to give equal statistical impact across datasets

SAMPLING — Nested sampling (*nautilus* Lange 2023)

Gaussian likelihood

$$\log L = -\frac{1}{2}\sum_i \left(\frac{(x_i - \mu_i)^2}{\sigma_i^2} + \ln(2\pi\sigma_i^2) \right)$$

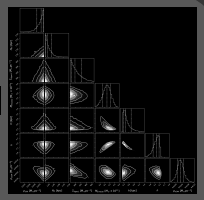

RESULTS

Einasto

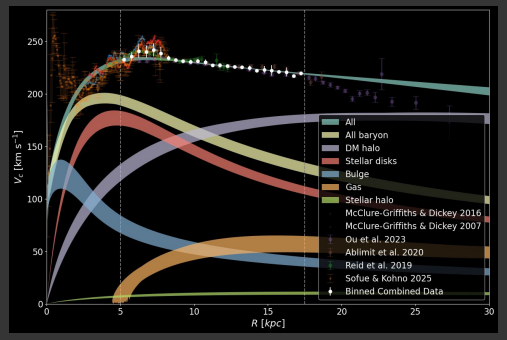

NFW

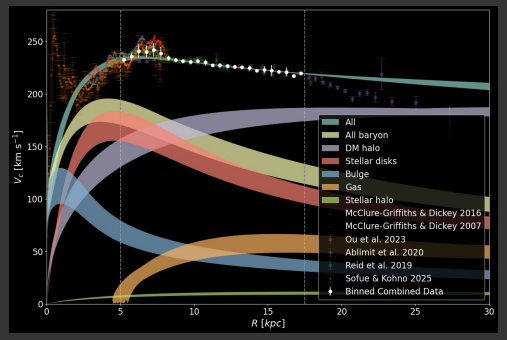

NFW DM Halo	r_s	kpc	$12.61^{+1.37}_{-1.55}$	–
NFW DM Halo	M_{NFW}	$M_\odot \times 10^6$	$17.91^{+5.44}_{-3.23}$	–
Einasto DM Halo	M_{Einasto}	$M_\odot \times 10^{11}$	–	$3.73^{+0.40}_{-0.43}$
Einasto DM Halo	h	kpc	–	$0.43^{+0.31}_{-0.13}$
Einasto DM Halo	n	–	–	$2.21^{+0.15}_{-0.23}$

Local density DM

Einasto

0.0104 ± 0.0002 M⊙ pc^{-3}
(0.395 ± 0.008 GeV cm^{-3})

NFW

0.0102 ± 0.0003 M⊙ pc^{-3}
(0.387 ± 0.011 GeV cm^{-3})

LITERATURE COMPARISON

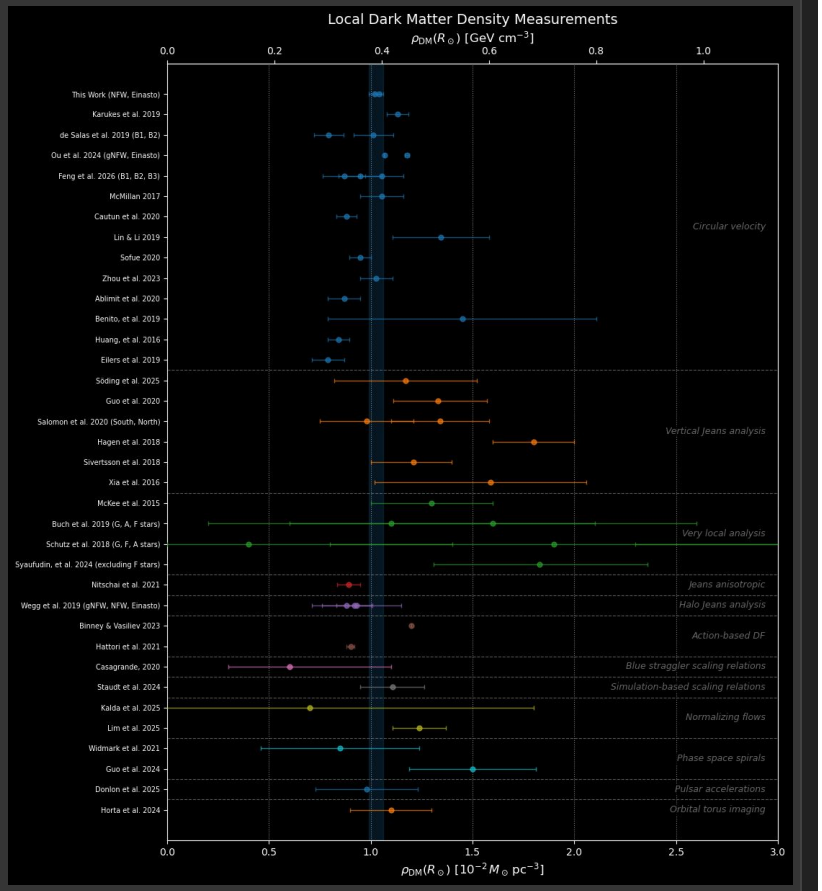

Lutsenko et al. 2026 (in prep.)

Email:
artem.lutsenko
@studenti.unipd.it

1st BiCoQ Conference: from gravity to particles

TOPOLOGICAL SIGNAL DETECTION IN LISA: A NOISE-AGNOSTIC APPROACH TO GRAVITATIONAL WAVES ANALYSIS

Lorenzo Viganò, Riccardo Buscicchio, Alberto Sesana, Massimo Dotti

Time domain data → **Embedding** → **Topological classification** → **Rapid parameter estimation without PSD assumptions**

Signals + **Noise** = **Data**

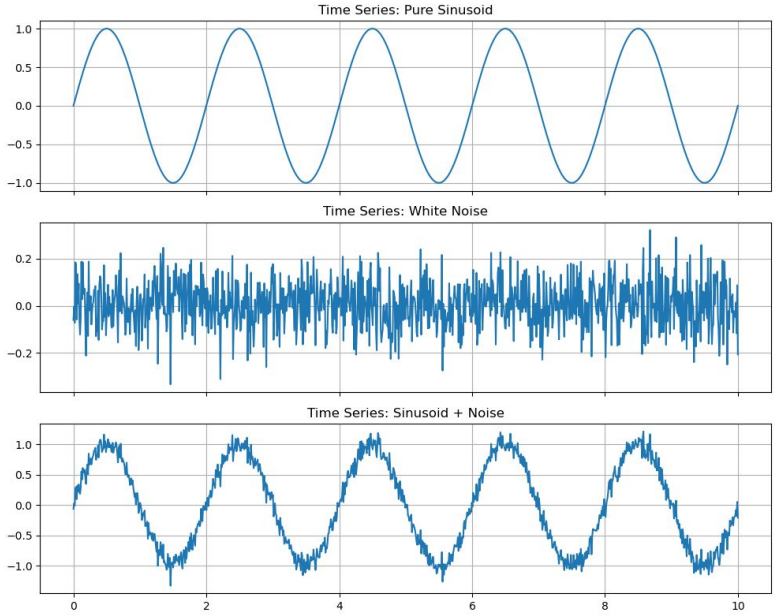

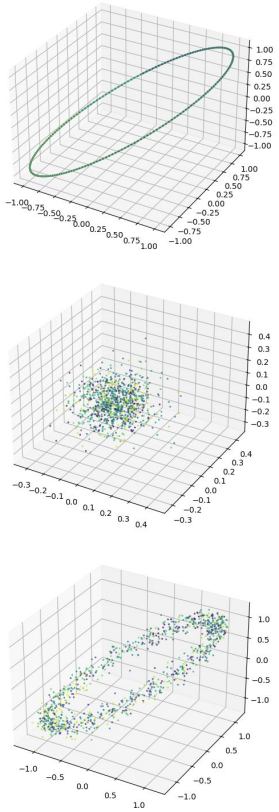

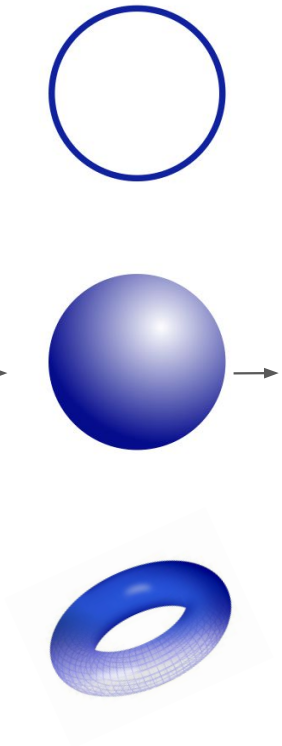

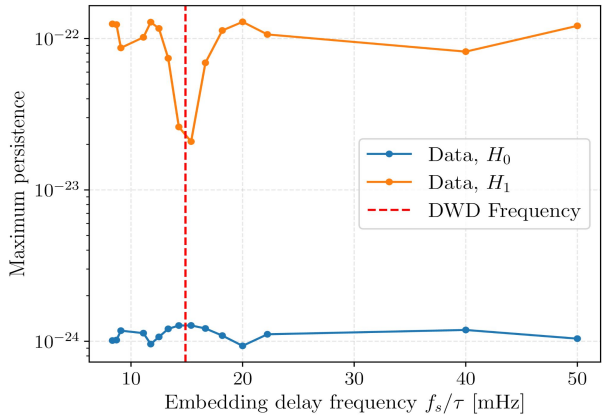

contacts

Realistic Beams, Non-Ideal HWPs: Quantifying Systematics and Cosmic Birefringence for Next-Gen CMB Cosmology

Author: Matteo Billi
matteo.billi2@studio.unibo.it

BICOQ
Centro Bicocca di Cosmologia Quantitativa

Next-generation CMB experiments are designed to measure CMB polarisation with unprecedented precision, targeting new physics beyond the Standard Model, like the **Cosmic Birefringence effect**. Achieving these goals requires exquisite control of instrumental systematic effects. Therefore, it is crucial to quantify the impact of **realistic Beam and Half-Wave Plate (HWP) systematics** for future data.

beamconv: TOD WITH REAL HWP AND FULL-SKY BEAM CONVOLUTION

beamconv

FIRST TIME-DOMAIN SIMULATIONS THAT INCLUDE BOTH HWP NON-IDEALITIES AND REALISTIC FULL-SKY BEAM CONVOLUTION

Open-source spherical harmonic beam convolution algorithm

- **Harmonic** representations of the polarised **beam** response and **sky** to generate simulated CMB **time-oder data**
- **Arbitrarily shaped beams**
- **Real HWP modulation**

STEP FORWARD IN MODELLING HWP SYSTEMATICS:
STANDARD TOD SIMULATION FRAMEWORKS SUCH AS SOTODLIB (SO) AND LITEBIRD_SIM (LITEBIRD) ACCOUNT FOR THE COUPLING BETWEEN BEAM RESPONSES AND IDEAL HWP MODULATION

CONTAMINATION OF THE BB POWER SPECTRUM

TOD simulation of a two-lens refractor telescope with (achromatic) HWPS and PO beam

HWP MUELLER MATRIX

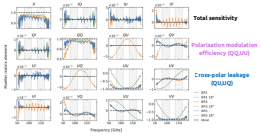

BEAM PROFILE

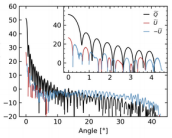

RESIDUAL BB SPECTRA

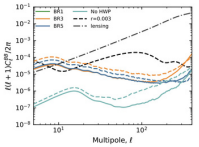

HWPs RESIDUALS COMPARABLE TO THE B-MODE AMPLITUDE WITH r=0.003

IMPACT OF HWPS NON-IDEALITIES ON CB ANGLE

Investigating the impact of realistic HWP systematics on isotropic CB using beamconv simulations.

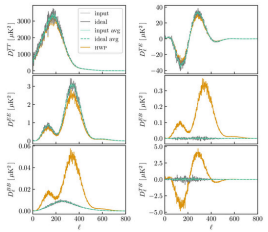

SIMULATION SETUP:
2-year satellite LiteBIRD-like scanning with 160 detectors at 140 GHz

HWP NON-IDEALITIES INDUCES A MISCALIBRATION POLARISATION ANGLE WHICH CAN MIMIC CB

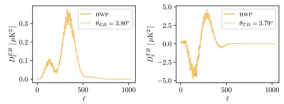

BEAM SYSTEMATICS within SO and LiteBIRD collaborations

TIME-ORDERED DATA (TOD) BEAM-CONVOLVED SIMULATIONS USING THE *SOTODLIB* AND *LITEBIRD_SIM* FRAMEWORKS
we utilise **4Π beam convolution to simulate TODs** and compare arbitrary beams with Gaussian models: this approach enables us to isolate and **quantify beam-induced systematics**

SO LAT: MAIN BEAM SYSTEMATICS

RESIDUALS POWER SPECTRA FOR LAT WAFER 13 AT 150 GHZ

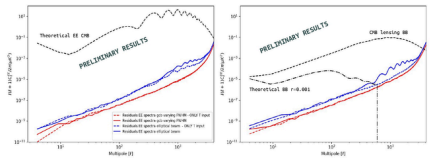

LITEBIRD MDR2 SIMS: FSL BEAM SYSTEMATICS

RESIDUALS POWER SPECTRA vPOSTKDP2 Option1

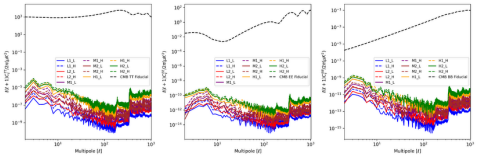

Anisotropic Cosmic Birefringence with Planck data and future forcasts

SATs-like and LiteBIRD-like forecasts

Application of this approach to forecast **constraints** on the **CB spectrum** for next-generation CMB experiments: simulating observations with a null intrinsic signal and a **white noise level of 2 μK-arcmin**

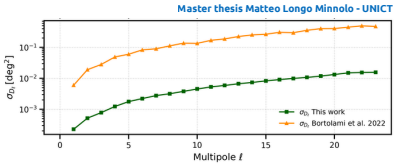

COMPARISON WITH THE PLANCK DATA UNCERTAINTIES: CRITICAL INCREASE IN THE CONSTRAINING POWER

INSTRUMENTAL SYSTEMATICS ON ANISOTROPIC CB

IMPACT OF EXTENDED FSL ON ANISOTROPIC CB MEASUREMENT

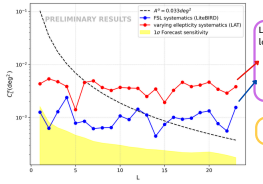

Level of systematic evaluated by applying the localisation of the D-estimators to the output maps:

- red line: LAT systematics due to 5% beam ellipticity variation across the focal plane;
- blue line: LiteBIRD systematics due to beam toy model with FSL.

Forecasts for Future LiteBIRD-like experiments (white-noise 2 μK-arcmin - Longo's thesis)

TESTING PRIMORDIAL NON-GAUSSIANITY ESTIMATORS IN NON-TRIVIAL COSMIC TOPOLOGIES

Primordial non-Gaussianity

↓

constrained through the non-linearity parameter f_{NL} using KSW estimator

↓

assumes statistical isotropy

Non-trivial cosmic topologies

↓

break isotropy and induces off-diagonal harmonic correlations

↓

potentially affecting the behaviour of standard isotropic estimators

Goal of the project: investigate how robust standard isotropic estimators remain when applied to CMB maps generated in topological universes.

Emanuela Sireno
MSc student in Astrophysics and Space Physics
University of Milano-Bicocca

Supervisors
Martina Gerbino, Massimiliano Lattanzi
INFN – Ferrara

Step 1 — Validation of the KSW estimator on standard Gaussian and non-Gaussian ΛCDM simulations

Step 2 — Application to topological CMB realizations: CMBtopology code used to generate Gaussian CMB realizations for the E1 and E3 topologies and analyzed them using the standard isotropic KSW estimator.

Any non-zero reconstructed f_{NL} would indicate an effective response of the isotropic estimator to topology-induced anisotropies rather than genuine primordial non-Gaussianity.

What happens when an estimator designed for an isotropic Universe is applied to a Universe that is not statistically isotropic?

Measuring the Cosmic Redshift Drift with the VLT: A Long-Term ESPRESSO Program into the ELT Era

Andrea Trost (atrost@sissa.it)
and the ESPRESSO WG4

In an accelerated expanding Universe, redshift of fixed objects changes with time

$$\dot{z} = (1+z)H_0 - H(z)$$

$\dot{z}_{z=4} \sim 10^{-11}$ yr^{-1} $\qquad$ $\dot{v}_{z=4} \sim 0.5$ cm s^{-1}yr^{-1}

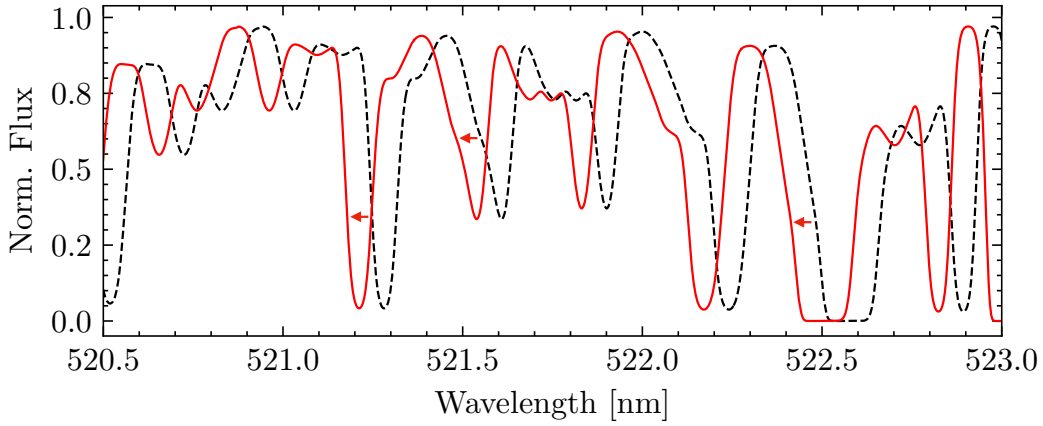

Direct, real-time, **model-independent** cosmological measurement

Use the Lyman-α forest as a tracer

But the measurement is **EXTREMELY CHALLENGING!**

These two are 8 million years apart…

Measuring the Cosmic Redshift Drift with the VLT: A Long-Term ESPRESSO Program into the ELT Era

Andrea Trost (atrost@sissa.it)
and the ESPRESSO WG4

Extreme long term *precision*, *accuracy* and *stability* are a must!

First ever dedicated experiment at high-z

First constraints + study of systematics

Stable Laser Frequency Combs are essential

ESPRESSO is competitive with next-gen facilities

Will lead the Redshift Drift Experiment in the next decades

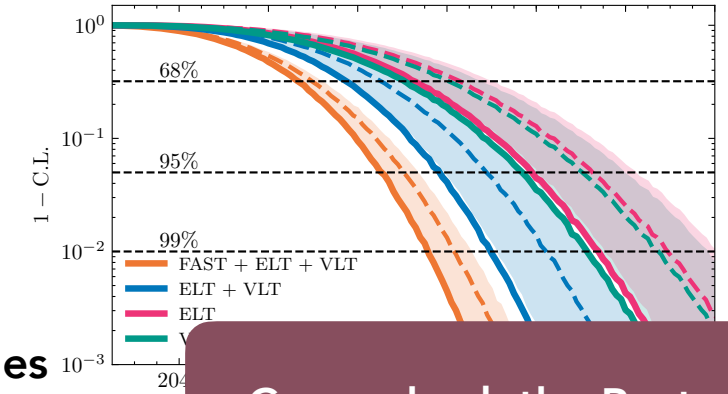

Come check the Poster!

Characterization of SiO_2 crystals for a multimode gravitational wave antenna

Riccardo Maifredi on behalf of the BAUSCIA experiment

First BicoQ Conference: from Gravity to particles

Strain sensitivity

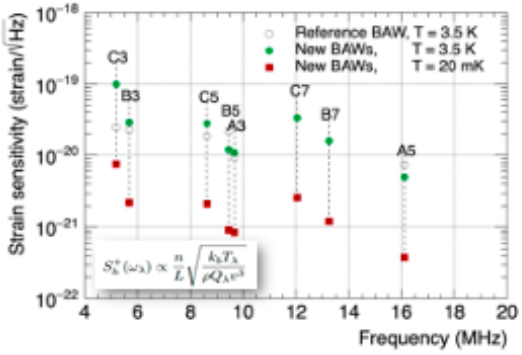

Putative Sources

- **PBH-PBH mergers** (G. Franciolini et Al. Phys. Rev. D 106, 103520)
- **Axion clouds collapse into MBH** (A. Arvanitaki et Al., Phys. Rev. D 83, 044026)
- **Phase Transitions in nascent NS** (K. Bleau et Al., arXiv:2603.18153 (2026))
- **QCD phase transitions following NS mergers** (D. Blas et Al., Phys. Rev. Lett. 136, 101401)

Readout scheme

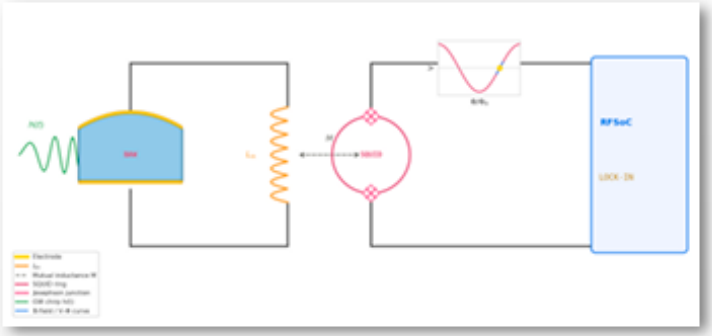

BAUSCIA dedicated dilution cryostat

Rakon Commercial Crystals for the BAUSCIA experiment

❖ Commercial crystals characterisation

The resonator characterisation relies on impedance measurements performed through a calibrated Vector Network Analyzer (VNA). For example, the VNA can be coupled to the resonator in a reflection geometry, with one electrode connected to one port and the other to ground.
A typical resonance scan is shown. Resonators' quality factors are derived from the unfolding of the coupling coefficient and stand at 10^7 at T = 4K.

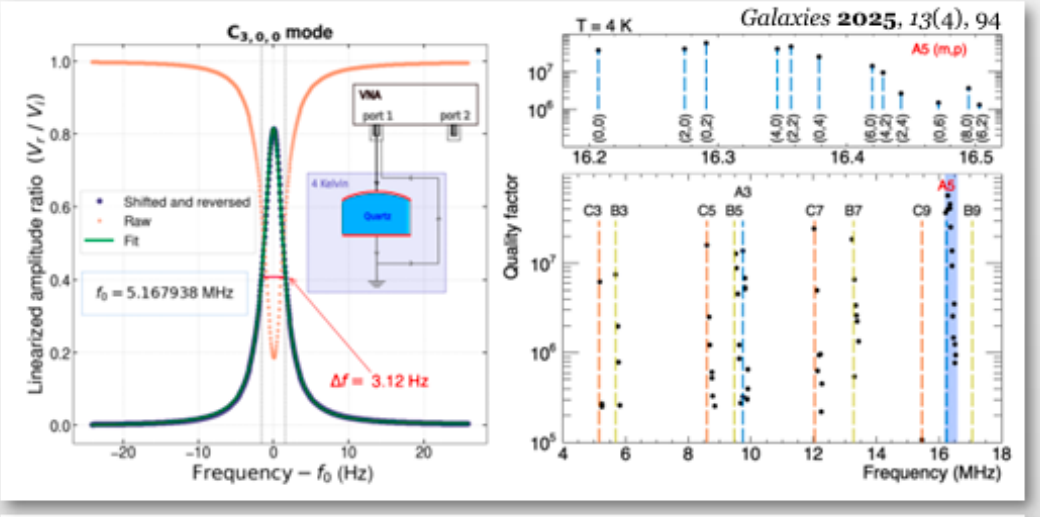

Galaxies **2025**, *13*(4), 94

$$f_\lambda \sim n f_{\{X,1,0,0\}} + \frac{n-1}{2}(\Delta f_x + \Delta f_y) + m\Delta f_x + p\Delta f_y$$

❖ BAW modes thermal noise assessment

A study of BAW mode thermal noise has been performed. In the left panel below, a resonance mode temperature dependence is shown.
The mode temperatures have been measured by fitting the resonance profiles as a function of the cryostat plate temperature.
As shown in the bottom-right panel, the mode temperatures and the cold plate temperatures show a strong linear relationship.
The motional resistance values extrapolated from the linear fit are in good agreement with independent measurements.

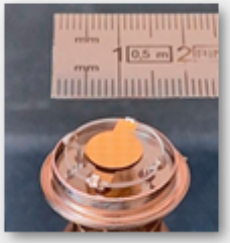

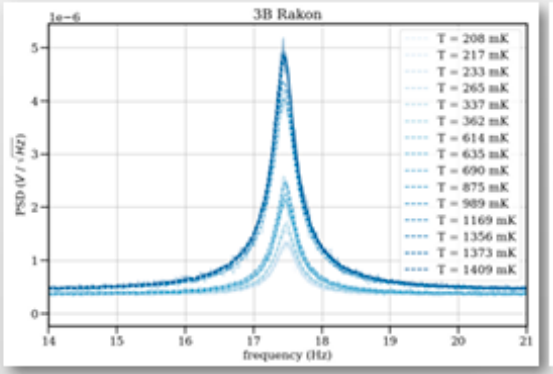

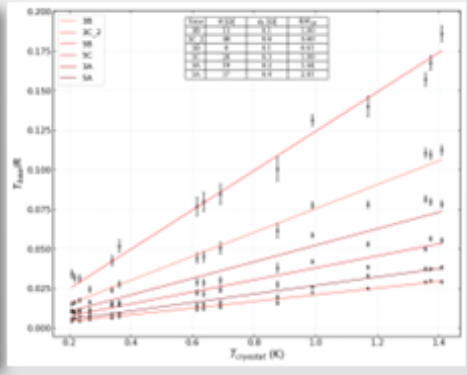

$$S_{vv}(\omega) \approx \frac{(M_{in} G V_\Phi)^2 4 K_b T R_\lambda}{\left| R_\lambda + j\left(\omega(L_\lambda + L_{in}) - \frac{1}{\omega C_\lambda}\right)\right|^2}, \quad \text{for } \omega \ll 2\pi \times 200\text{MHz}$$

Ready for Data Taking!
(Summer 2026)

Custom Crystals R&D

❖ Room temperature characterisation

Two SC-cut quartz crystals with thicknesses of 9,13 mm were characterised at room temperature in vacuum via a transmission measurement performed with a VNA. A fit of every resonance was performed leveraging the Butterworth-Van Dyke electrical model in order to extract resonance parameters.

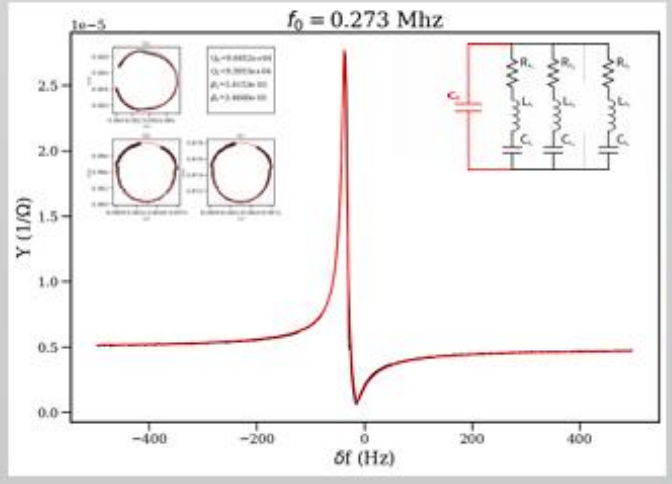

❖ Strain sensitivity optimisation

The crystal's top surface geometrical profile acts as a **potential barrier** which governs how well phonons are trapped inside the bulk of the crystal.

$$\frac{\partial^2 \mathbf{u}}{\partial t^2} \approx c_l^2 \nabla(\nabla \cdot \mathbf{u}) - c_t^2 \nabla \times \nabla \times \mathbf{u} \longrightarrow \delta f(r,\theta) = \left[-\frac{c_t^2}{2\omega_n^2} \nabla_\perp^2 + \frac{\hbar \omega_n^2}{L_0} \Delta(r) \right] f(r,\theta)$$

By optimising the top surface geometrical properties, it is possible to trap phonons of the first overtone of the resonant modes, enhancing strain sensitivity.
Inspired by the work of T.Trickle (T. Trickle, Phys. Rev. D **112**, 055043, 2025), we have numerically solved the acousto-elastic wave equation, gaining knowledge on the phonon distribution for different geometrical cuts.

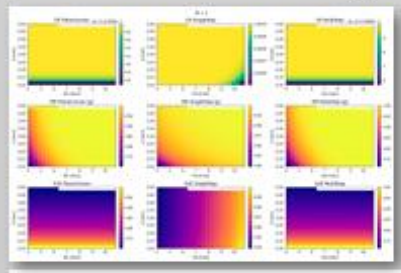

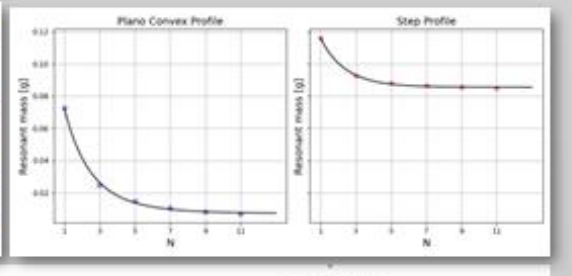

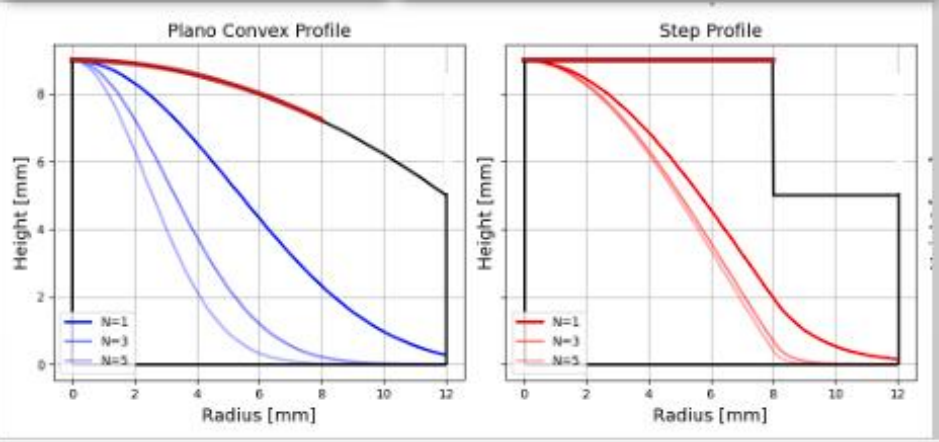

Outlook and future prospects for BAUSCIA